A case study on the application of destructive and non-destructive methods for evaluating jet-grouting column integrity for bridge-pier scour protection (Cuneo, NW Italy)

A CASE STUDY ON THE APPLICATION OF DESTRUCTIVE AND NON-DESTRUCTIVE METHODS FOR EVALUATING JET-GROUTING COLUMN INTEGRITY FOR BRIDGE-PIER SCOUR PROTECTION (CUNEO, NW ITALY).

S. Bonetto[1], C. Colombero[1], C. Comina[1], N. Giordano[1], A. Giuliani[2], G. Mandrone[1], S. Nicola[3] and P. Tible[3]

1 - Dipartimento di Scienze della Terra – Torino University, Via Valperga Caluso, 35 – 10125 Torino (IT).

2 - AG3 srl – Spin Off Company of Torino University, Via Valperga Caluso, 35 – 10125 Torino (IT).

3 - Provincia di Cuneo, Direzione Mobilità ed Infrastutture, Settore Viabilità, Corso Nizza, 21 – 12100 Cuneo (IT).

Corresponding Author

Giuseppe Mandrone
Via Valperga Caluso, 35 – 10125 Torino (IT)
giuseppe.mandrone@unito.it
tel: +39 011-6705113

Abstract

A case study on the use of direct and indirect investigations for the effectiveness evaluation of jet-grouting interventions for bridge scour protection is presented. The major concern of this scour countermeasure is that a reliable verification and imaging of the exact dimensions and shape of the grouted elements and their related strength and integrity are difficult to obtain. An integrated cost-effective e and slightly invasive approach, by means of indirect surveys, is proposed in this work to limit re-drilling and core sampling of jet columns. Tests are performed on a bridge located in the Province of Cuneo (NW Italy). On site, active fluvial activity was scouring four of the nineteen bridge piers and jet-grouting interventions were designed to prevent bridge collapse. A dual approach was consequently applied to evaluate the goodness of jet-grouting treatments: results of direct tests (visual and mechanical characterization of core drillings, with Point Load and Uniaxial Compressive Strength tests) have been compared to indirect investigations (seismic down-hole tests and 2-D cross-hole tomography, laboratory Ultrasonic Pulse Velocity measurements). All the techniques showed potentiality in identifying variations of the jet-grouting properties within the columns. Generally, worsening in jet-grouting properties was coherently identified by a decrease in the seismic velocities and in the mechanical parameters and confirmed by visual inspection of core drillings. Local anomalies and discrepancies between the adopted method were however highlighted and critically discussed as a function of the limitations, disturbances and investigated volumes of each method.

Keywords: Direct investigation, Geophysical methods, Bridge scour, Jet grouting, Quality assessment.

1. INTRODUCTION

Bridge scour is the predominant cause of bridge failures. It consists of a dynamic phenomenon, related to the erosive action of flowing water and occurs around piers and abutments. Scour depends on several factors, such as water depth, flow velocity, pier shape, channel protection measures and sediment type. It can be predicted and taken into consideration in the bridge design phases by accounting for all the key factors causing the phenomenon. This can be performed by adopting empirical equations or by modeling the process with numerical or laboratory approaches (Deng and Cai 2010). However, scour design has only recently become a standard practice. Most of the oldest bridges were not specifically designed with proper scour countermeasures. In the field, there is consequently a need for proper monitoring activity on structures potentially affected by scour. In the last two decades, several authors have employed surface geophysical methods to evaluate the progression and dimension of the phenomenon around piers. Adopted techniques involve radar (Millard et al. 1998; Park et al. 2004), sonar (Hayes and Drummond 1995; De Falco and Mele 2002), combined seismic refraction and refraction microtremor (Rucker 2006), electrical resistivity (Gemmi et al. 2003; Santarato et al. 2011) and induced polarization measurements (Tucker et al. 2015).

In addition, several techniques and methods can be adopted to mitigate the scour risk and improve the overall structure performance. Armouring or flow-altering countermeasures can be applied by adding a resistant layer around the pier, in the first case, or by changing the hydraulic properties of the stream by means of spur dikes, guide banks, parallel walls or collars (Lagasse et al. 2007; Barkdoll et al. 2007). In this context, jet-grouting protection measures are widespread, because they can be easily implemented near already-existing foundations (Croce et al. 2014).

Jet grouting consists of a modification of the soil that, among other applications, can be used for consolidation of the natural underground for stability purposes. Pre-designed volumes of grout/water mixtures are injected into the ground, adjusting the pressure, injection rate and duration of the activity. The jet-grouting column integrity and cementation degree are the key aspects determining the effectiveness of the intervention. Because grouting injections cannot be controlled precisely, a successive quality control is essential. Consequently, the major concern of the treatment effectiveness verification is to obtain a reliable imaging of the exact position and shape of the grouted element. Classical methods to verify the quality of injections consist of re-drilling the modified ground at selected points to check the mechanical quality of the barrier by means of direct methods, such as Point Load tests or Uniaxial Compressive Strength (UCS) tests on core samples. However, this method is expensive, and it partially worsens the structural performance of the intervention, while providing only localized results.

In contrast, geophysical methods are an example of non-invasive, low-cost and less-time-consuming investigations. When using geophysical methods for jet-grouting effectiveness evaluation, a preliminary evaluation of the natural ground (before the intervention) is usually performed. As an example, Gemmi et al. (2003) carried out both surface and cross-hole ERT (Electrical Resistivity

Tomography) to ascertain the geotechnical characteristics of the natural soil and then check the integrity and continuity of some jet-grouting test columns drilled in the same material. This technique was found to be a valid tool for imaging the migration of the grout. Padura et al. (2009) applied seismic techniques (cross-hole and down-hole) to determine the consolidation degree achieved in the foundation soil of an ancient building in Granada (Spain) that was reinforced by cement-bentonite jet-grouting injections. Seismic surveys were conducted before and after the treatment to check the efficiency of the intervention by identification of the improvement in the dynamic stiffness modulus.

Even when a preliminary evaluation is not possible due to technical or economic issues, geophysical methods can be useful both to extrapolate the results of local direct tests and to investigate wider grouting volumes in a non-destructive manner. To infer the volumetric improvement in geotechnical behaviour caused by jet-grouting intervention, seismic tomography can be used to visualize and quantify the distribution in compressional (P) and shear (S) wave velocities. The velocities of elastic waves (Vp and Vs) are a widely accepted parameter correlated with the structural condition of concrete-soil mixtures. In this respect, a similarity between seismic surveys and direct (Point Load or UCS) tests can be stated: both methodologies are essentially devoted to the evaluation of the mechanical consistency of a grouted volume. Correlations between seismic velocities and UCS have been proposed for various rock types (Barton 2007).

The possible use of drilling boreholes for seismic sources and receivers (cross-hole tomography) is recommended in this working contexts because it is expected to provide higher-resolution imaging compared with surface-based seismic methods. In particular, the resolution of cross-hole tomography is not depth-limited, since most of the energy travels between the holes so that a trans-illumination of the imaged medium can be achieved. The first-arrival travel times are then used to produce a tomographic velocity cross-section of the subsurface between the two boreholes.

In addition, ultrasonic measurements performed directly on site or on selected samples, have been proven to be successful in both the evaluation of concrete and geothermal grouting properties and the determination of continuity and quality of a cement pile (Colombero et al. 2016).

In this paper, a case study involving direct and indirect investigations devoted to the evaluation of a jet-grouting intervention is presented. The effectiveness of several investigation techniques was evaluated on a bridge crossing a river where active fluvial activity was scouring four of the nineteen bridge piers and strongly affecting their integrity and stability. Seismic methods were applied on site. A traditional laboratory approach with direct tests (Point Load and Uniaxial Compressional tests) and geophysical measurements (Ultrasonic Pulse Velocity, UPV) on samples collected from continuous core drillings was then used to have direct control and validation on the measured field parameters. The different methodologies were finally compared to verify their efficiency and role in an integrated less-expensive and only slightly-invasive approach for the verification of column integrity.

2. THE CASE STUDY (CUNEO, NW ITALY)

The study area is located in the Province of Cuneo (NW Italy, Figure 1a), 100 km South of Torino, in the high Po Plain. The bridge of a provincial street (*SP3*) crosses the Stura di Demonte River at N391436.727 E4922867.766 (WGS84 UTM32N), at an altitude of 420 m asl. The bridge is 583 m long and supported by 19 piers with a constant spacing of 28 m.

Geologically, the site is characterized by thick (60-70 m) quaternary fluvioglacial and alluvial deposits of continental origin, laying on transitional *facies* between marine and continental environments (50-60 m). The younger unit (Pleistocene inf. – Holocene) is characterized by pebbles and gravels in a sandy matrix with rare silts; the older unit (Pliocene med. – Pleistocene inf.) consists of alternating sands and silts due to the progression and regression of the coastal line in the late Pliocene. In the studied area, quaternary sediments are covered by the actual principal alluvial complex, which consist of two sub-units. The shallower one is represented by coarse-grained gravels (pebbles and boulders, with Ø up to 1 m, of various lithology, mainly limestone and gneiss) in a sandy matrix (Figure 2), with local presence of prevalent sandy deposits. The second sub-unit is distinguished by the abundance of fine-grained matrix that increases with depth. These sediments are very permeable (hydraulic conductivity $K=10^{-3}$–10^{-4} m/s) and host the shallow groundwater, which is directly connected to the river flow.

Near the bridge, the Stura di Demonte River is characterized by multiple braided channels (Figure 1b) with a riverbed that is approximately 150 m large and river banks approximately 500 m away from each other. Following a heavy-rainfall event in March 2011, fluvial activity affected the stability of 4 foundation piers located in the middle of the bridge (P8 to P11, Figure 1c and Figure 2). A stabilization intervention was therefore planned to reinforce the stability of these central piers. Collars of 64 reinforced jet-grouting injections (at a spacing of 0.65 m) were designed all around the abutments of each pier to strengthen the foundations with a 0.8-m-thick and 9-m-deep barrier of consolidated soil. On the top, these columns were linked with a concrete kerb (Figure 3a).

3. MATERIALS AND METHODS

A dual approach, based on both direct and indirect investigation methods, was applied to evaluate the effectiveness of the jet-grouting treatment and to test the integrity and lateral continuity of the gravel-concrete columns. Direct tests involved the realization of continuous core drillings of the grouted columns at three different corners of each pile (Figure 2 and Figure 3b) to an average depth of 10 m. Drilling cores were analyzed and described to distinguish levels with different grain sizes and cementation and for a visual inspection of the treatment. Samples of the drilled cores were collected for laboratory characterization using UPV measurements, Point Load and Uniaxial Compressive tests. The boreholes were subsequently used for indirect investigation using geophysical methods. A seismic survey was performed on each pile, using surface and in-hole sources and receivers. Seismic acquisition geometries for down-hole and 2-D cross-hole tomography interpretation were deployed.

3.1 Continuous drilling campaign

Borehole tests were realized with a continuous-coring method, allowing for direct analysis and classification of the obtained cores. Coarse grain sizes (gravels and pebbles) were dominant in the cores, but thinner grain sizes (sands and silty sands) were also present. Levels with different grain sizes and degrees of cementation were recognized, and consequently five different material classes (from A to E) were assigned to the different portions of the cores. Samples for laboratory characterization and testing were collected from approximately each core meter, or denser where variations of the material class occurred.

3.2 Seismic survey

A seismic survey, combining surface-based and cross-hole seismic tomography for P and SH waves, was designed for each pier. In Figure 4, an example of the adopted acquisition scheme is reported for the investigated pier (P10) of which results will be presented in the following. Acquired data provided P- and SH-wave velocity imaging along two perpendicular seismic sections (NE-SE and SE-SW), as highlighted in Figure 2 and Figure 3b.

A prototype string equipped with 8 three-component geophones (10 Hz) at 1-m spacing, stiffly connected by an aluminium bar that controls the orientation of the geophones in the borehole, was used in the three test boreholes of each pile. A sledgehammer, impinging both vertically and horizontally on a steel rod, provided the surface source for P- and SH-wave generation at different locations along the lines connecting the three holes (Figure 4). For SH-wave source polarity inversion was adopted to improve the reliability of first break picking (Figure 5). The first part of the survey involved only surface shots for P and SH waves at different locations on the line connecting SE and NE boreholes (long side), with geophones recording first in the NE and then in the SE borehole, followed by analogous acquisitions on the line connecting SE and SW boreholes (short side), with geophones recording first in the SE and then in the SW borehole. The traces related to the shots closest to the three boreholes, were used for down-hole data interpretation. A Borehole Impacter Source by Geotomographie GmbH was then used as an in-hole source in the SE borehole at different locations, from 2- to 9-m depths. Acquisitions of the in-hole generated signal were made with in-hole geophones in both the SW and NE holes. For all the tests, seismic traces were recorded with a window length of 500 ms and a sampling interval of 31.2 μs. For each shot, more than 10 recorded traces were stacked to increase the signal-to-noise ratio.

Seismic surveying at the site turned out challenging due to the significant presence of noise, coming both from traffic on the bridge and from jet-grouting and drilling operations in the nearby piles that were often in progress during the seismic tests. Natural noise resulting from a considerable flow rate of the river summed up to these anthropic sources. These acquisition conditions resulted in an overall poor quality of the acquired seismic traces (particularly for the ones with far shot positions), which need to be analyzed from a critical point of view but are however inevitably and commonly

affecting similar testing situations. Examples of P and SH seismic traces acquired in the NE borehole of the investigated pier are reported in Figure 5, for two different shot positions highlighted in Figure 4 (A and B). A clear deterioration of the seismic signal quality with increasing distance of the source (from A to B) is noticed in the traces, which affects the reliability of first-break picking for the distant shots.

All the arrival times, picked on the seismic traces from surface and in-hole shots, were inverted to achieve a tomographic cross-hole image of the investigated volume with the use of GeoTomCG software, which performs three-dimensional tomographic analysis with any source and receiver positions in a 3-D grid. The software allows for curved-ray calculations, which have been observed to be more accurate in cases of strong velocity contrasts. Curved ray tracing is performed with a revised form of ray bending, derived from the method of Um and Thurber (1987). Inversions are performed with the Simultaneous Iterative Reconstruction Technique (SIRT, from Lytle et al. 1978 and Peterson et al. 1985).

3.4 Ultrasonic Pulse Velocity measurements of core samples

Core samples from the continuous drillings were selected for laboratory measurement of Ultrasonic Pulse Velocity (UPV). Tests were conducted on a total of 26 samples, attempting to follow as closely as possible the requirements of the ASTM D2845-08 Standard for Laboratory Determination of Pulse Velocities (ASTM 2008). The investigated samples were representative of the various degrees of variability visually observed along the drillings (material classes A-D). Callipers were used to accurately measure the width, length and thickness of the samples in accordance with the aforementioned specifications. The main cause of difficulty in maintaining the testing limits within the ASTM standards was related to the relevant grain size of some portions of the grout columns. The mean grain dimensions (d) were indeed not always below the suggested limits of sample lengths (i.e., length $\geq 10d$).

An ultrasonic pulse generator (Pundit Lab, PROCEQ), that provides pulse emission and acquisition, was combined with two cylindrical transducers having a nominal frequency of 54 kHz to perform the measures. The travel time of the ultrasonic pulse across the sample is simply based on the time lapsed from the signal emission and reception, and since the distance is known, the determination of the UPV is straightforward. The signals were sampled with a frequency of 2 MHz. For each sample, the acquisitions were repeated 4 times to obtain several stable traces and verify the repeatability of the measurements. Manual picking of the first arrival time was performed on each recorded trace to obtain the travel time along the investigated distance.

3.5 Point Load Test and Uniaxial Compressive Strength

The Point Load test was performed on a total of 64 samples selected from the from drilled cores, following to the Suggested Method for Determining Point Load Strength (ISRM 1981; ISRM 1985; ASTM 2002) and making use of the diameter-corrected Point Load Index (I_{S50}) and a proper calibration

factor (k). More than one specimen was tested in the case of a sufficiently long drilling core assigned to the same material class. The applied force at failure (P) for each sample was processed for the definition of the Point Load Index I_S, obtained by the ratio between P and the equivalent diameter of the core (D_e):

$$I_S = \frac{P}{D_e^2} \quad (1)$$

Because I_S depends on the diameter of the sample, it was corrected to obtain the equivalent value representative for a 50-mm-in-diameter core (I_{S50}) (following Equation 2), which is directly correlated with the Uniaxial Compressive Strength of the sample (Equation 3).

$$I_{S50} = \left(\frac{D_e}{50}\right)^{0.45} \cdot I_S \quad (2)$$

$$UCS = k \cdot I_{S50} \quad (3)$$

Data were then grouped as a function of the material class. Following ISRM suggestions, the two lowest and highest values obtained for the same class where rejected. The remaining values were averaged to obtain the mean value and the standard deviation for each class. Experimental studies on various rock types from different areas of the world have resulted in various value ranges for k. The ISRM (1985) suggests a k-range between 15 and 50, especially for anisotropic rocks; Bowden et al. (1998) reported that k is not a unique value, even for a single set of specimens but is strength-dependent. Singh et al (2012) recently recommended a conversion factor of 21–24 for hard rocks and 14–16 for soft rocks, whereas Jahanger and Azad Abbas (2013) proposed a k of approximately 6 for rocks with very low strength (≤27.5 MPa). Finally, Zacoeb and Ishibashi (2009) analyzed the correlation between UCS and I_{S50} in the case of concrete with specific features in terms of grain size of the aggregate.

In the current application, jet-grouting technique generates an artificial conglomerate by means of cement injections in a natural alluvial deposit composed of gravel, pebbles and blocks of various lithology and size (up to various decimetres). In this case, a unique correlation factor between UCS and I_{S50} is difficult to estimate because it depends on the size and composition of the pebbles, their degree of alteration, the strength contrast between block and matrix (Sonmez et al. 2006), the volumetric block proportion (VBP) and their orientation with respect to the stress (Kahraman and Alber 2006). Consequently, following literature suggestions and considering the UCS values obtained from uniaxial compression laboratory tests accomplished on the same material classes, different k factors were assigned to each class.

These reference UCS tests were performed on 9 samples selected from the drilled cores, following to the ISRM recommendations and ASTM Standard Test Method for Unconfined Compressive Strength of Intact Rock (ISRM 1979; ASTM 2002). Unfortunately, sample length was unable to respect the length-to-diameter ratio of 3 to 1. All test samples were cylinders with a diameter of 107 mm, and lengths ranging between 78 and 122 mm, resulting in length-to-diameter ratios between 0.7 and 1.1. For these reasons, samples were not rectified and cored but directly loaded using a servo-controlled 500-kN testing machine (Baldwin – Zwick, B1058 Series MA model). All samples were loaded at a controlled strain rate of 0.05 $(N/mm^2)/s$ until sample breakage.

4. RESULTS

4.1 Continuous Drilling campaign

Examples of the five different material classes identified on the basis of grain size and degree of cementation are reported in Figure 6. In particular, the five identified classes were constituted by:

- A: cemented gravels and pebbles with no alteration;
- B: cemented altered gravels and pebbles;
- C: cemented sandy gravels;
- D: silty sands and silts with no cementation;
- E: gravels and pebbles with no cementation and poor matrix.

The identified material classes are representative of the possible variability within a jet-grouting column injected in the considered starting material. Therefore, similar subdivisions can potentially be applicable in other case studies. In particular, classes A and B should be considered as concrete-like materials with very coarse aggregate (greater than 40 mm). Class A is characterized by pebbles which are, according to their lithology and absent alteration, stronger than the matrix, whereas class B shows a stronger matrix and weaker pebbles due to their marked alteration degree. Class C is almost homogeneous in size and composition and can be associated with a sandstone. Material classes D and E are finally the ones in which jet-grouting treatments had ineffective results. However, these last material classes affect only approximately 15% of the entire set of investigated cores.

4.2 Seismic survey

In Figure 7, the results of seismic down-hole tests in the three boreholes of pier P10 are shown. Both true-interval velocity and average velocity interpretations are reported for P and SH waves. The average measured Vp value along the investigated columns is approximately 2 km/s. Local levels with lower velocities are found, especially in the SE borehole, where Vp decreases below 1 km/s between the depths of 4 m and 5 m. A general decrease in velocity is noticed at the end of all the boreholes, coherently with the end of jet-grouting columns. Conversely, higher Vp values (approximately 4 km/s) are present on top of the SW borehole and can be related to the presence of the concrete kerb. Vs profiles are in good agreement with Vp results along all the investigated boreholes.

The tomographic sections around the same pier, obtained by combining all the surface and in-hole sources and receivers, are reported in Figure 8. The variability in the seismic velocity field of P- and SH-wave sections are comparable. In all sections, the highest seismic velocities are found in the top portion (Vp and Vs of approximately 3 km/s and 2 km/s respectively). This part of the sections, as highlighted in Figure 8 (b and d), is the portion of grouted columns directly embedded in the reinforced concrete kerb foundation. Generally, in the shortest section (Figure 8, a and c), which is not completely affected by jet-grouting injections (see Figure 3), slightly lower velocities are found: an area with Vp of approximately 1 km/s is depicted and a similar velocity reduction, even if less marked, can be observed for SH waves. Globally, good jet-grouting conditions are observed in the injected zones. Local

variations, in terms of low-velocity zones, are observed, normally in a range of 25% from the mean value. These are particularly evident in the S-wave velocity section, where an area with velocities lower than 1 km/s is present (Figure 8d).

4.3 Ultrasonic Pulse Velocity measurements on core samples

Measured UPVs are summarized in Figure 9 for each material class. Most of the obtained velocities are consistent and indicative of a good-quality jet-grouting intervention. A decreasing velocity trend is observable as a function of the material class (from A to D). Indeed, coherently with the grain-size distribution and cementation of each material type, classes A and B show the highest velocity values (from 2 to 4.5 km/s). The higher variability of the results for class A can be related to the strong heterogeneity of the forming lithologies and to the relevant grain size of the elements. In these conditions, tested samples showed considerable structural heterogeneities linked to the local dominant presence of elements (gravel and pebbles) or matric (cement). UPV values below 2 km/s were measured on a small number of samples belonging to classes C (from 2 km/s to 1.8 km/s) and D (from 1.3 km/s to 0.5 km/s). It has, however, to be noticed that uncemented or scarcely cemented levels could not have been sampled properly for these tests. As a consequence, no significant information was retrieved for material class E.

Measured UPVs are generally slightly higher with respect to field seismic velocities. This can be explained by taking into account the higher testing frequency of ultrasonic tests and the different investigated volumes between field and laboratory measurements, with the predominant effect of the presence of relevant grains at the laboratory scale and, conversely, the smearing of the field velocities, which are averaged over wider investigation volumes.

4.4 Point Load Test and Uniaxial Compressive Strength.

As for UPV determination, most of the samples for Point Load and UCS tests belong to classes A and B and none to the E class, due to the impossibility of obtaining samples on this type of unconsolidated non-compacted material. Results of the mechanical tests were divided into the four classes (A, B, C, D) to estimate the average mechanical strength value for each material type (Figure 10). The average mechanical behaviour is quite good for classes A and C (I_{S50}>0.8), second-rate for class B (I_{S50}=0.57) and really poor for class D (I_{S50}<0.1). For the structurally similar classes A and B (cemented gravel and pebbles with clast-supported structure) the values are strongly conditioned by the quantity and dimension of pebbles, type and abundance of matrix, and uniformity coefficient. In class B, pebble alteration generally reduces the I_{S50} values. As for UPV measurements, structural variations between the samples of each class reflect the variability within the results of each material type, particularly for class A.

These observed I_{S50} values were later correlated by means of Equation 3 to UCS values. To do this, uniaxial compression laboratory tests on selected samples of classes A, B and C have been used as references to obtain the best calibrating factor (k) for each material class. In Figure 11, the results of this conversion are reported. It can be observed that, among the different classes, class C shows the best mechanical properties and lower internal variability. This is mainly related to the more homogeneous properties of jet-grouting columns in this material, since the results are not affected by clast heterogeneities (see Figure 6c). Seismic velocity measurements partially conflict with these results, highlighting lower velocities for this material class.

5. DISCUSSION

A comparison of the results yielded by the different techniques is reported in Figure 12 for the boreholes of the example pier P10. To understand the effectiveness of the different adopted techniques in identifying property variations along the columns, data are reported together with an adapted intensity scale. In particular, the material classes have been converted to numerical values, from best quality to worst (from A=5 to E=1, 1 step down for each material class), while UCS values retrieved from the Point Load Tests have been divided by 5. It is important to underline that, even if the techniques adopted for characterization are based on different physical properties, they are all devoted to the evaluation of the same aim: grouted-column mechanical integrity. Therefore, a useful comparison of the results is also able to analyze the effectiveness and cost convenience of the different methods.

From the combined analysis of the results, it can be observed that both on-site and laboratory techniques show potentiality in identifying the variation of jet-grouting properties within the columns. In particular, decreases in jet-grouting properties identified by negative variations of the seismic velocities for the down-hole test are coherently verified by direct inspection of core drillings (material class). As an example, in Figure 12a (SW drilling hole of P10), all of the methods are able to depict the abrupt parameter variation from the existing shallow bridge foundation to the grouted column at depth. Coherently with the statistical analysis of all the data, UPV measurements generally exhibit higher values with respect to field seismic data, probably linked to the higher frequencies of the ultrasonic probes. However, the general trends of the columns are correctly depicted by both techniques. Both methods indeed observe a reduction in velocity with depth (e.g., in Figure 12, b and c, SE and NE drilling holes of P10). It must also be considered that down-hole seismic tests investigate a wider volume of material with respect to ultrasonic measures on small samples. These last can therefore be influenced by the significant dimensions of clasts within the samples and result in higher local velocities. UCS values derived from the Point Load tests also agree with the general trends depicted by the other techniques. However, for them as well, localized anomalies could reflect the local presence of larger clasts (see the abnormally high UCS value in Figure 12b at a depth of 4 m) or predominant low-consistency matrix.

When seismic data are interpreted in a tomographic approach (Figure 8), local anomalies appear to be more smeared, and the resolution in identifying low-velocity layers observed in down-hole profiles appears reduced. It must be considered that seismic testing was particularly challenging in the proposed case study due to both noise disturbances (river water, traffic noise and injecting operations) and difficult ray coverage. The reliability of the low-velocity zones depicted in seismic sections must therefore be analyzed critically. In this respect, seismic rays tend to concentrate on the top of the sections due to the presence of the high-velocity concrete kerb and a reduction in ray coverage can be observed towards the bottom. Nevertheless, similar testing conditions are reasonably expected in comparable case studies. Possible alternative countermeasures for improving data quality in similar testing situations would imply to the reduction of external noise sources. This could be obtained by closing the road over the bridge to reduce traffic disturbance, interrupting jet-grouting injections at a distance of at least 100 m from the testing pier, and deviating the flow of the river far from the piles involved in testing. These strategies have, however, the shortcoming of being neither time- nor cost-effective. Post-processing of the seismic traces by frequency filtering has demonstrated as only partially useful in removing these external noise sources, since frequency bands of seismic signals and external disturbances are strongly superimposed.

Site conditions were, as a whole, particularly arduous also due to the type of material encountered by jet grouting: the presence of pebbles and large boulders implied lack of homogeneity in the injection of the cement and consequently made the geophysical acquisitions and direct surveys very complex. In principle, it is possible to observe good agreement between indirect and direct measures, even if differences between techniques highlight different aspects of the complex material/jet pile. For example, direct measures have been carried out on small samples (decimetre), while geophysical measures investigate portions of ground up to 10 m. Evidently, differences in the scale of observation cannot be neglected. In similar conditions, therefore, a statistical evaluation of a consistent number of samples is required to overcome heterogeneities related to the material. Given that scour problems are likely to affect rivers with high hydraulic energy and therefore relevant clasts dimensions in the deposited material, similar conditions are also expected in other similar case studies.

To establish a useful correlation between direct and indirect methods, contemporary measurements of seismic velocities (from down-hole and UPV tests) and Point Load results (converted to UCS) have been correlated. Only material classes A and B have been considered since the other material classes have too-reduced numbers of samples to establish a statistically reliable correlation. All the correlations between seismic velocity and UCS available in the literature for various rock types (Barton, 2007) are reported in the form of an exponential relation. In Figure 13, the obtained correlation ($UCS= 4Vp^{1.05}$) for the data of this work is shown. The reliability of the proposed correlation ($R^2=0.78$) is not particularly high, reflecting the high variability of Point Load and UPV data (see Figures 9 and 10). Nevertheless, the possibility of establishing similar correlations for similar case studies would have the benefit of reducing the number of sampling points and potentially directly transforming the imaged

2-D velocity sections in UCS sections. This transformation is not attempted in the present case study due to the aforementioned limitations in material class representativeness.

With respect to the cost-effectiveness of the entire survey in analogous contexts, an initial geophysical campaign should be suggested to provide general information on the proper execution of jet-piles. In addition, if significant anomalies are observed in the seismic sections, localized direct drillings with further laboratory tests on the core samples will clarify the success of the intervention. Following this practice would allow cost and time savings, positively influencing the overall management of the site and optimizing the final results. Indeed, costs for the execution of a single 2-D seismic section are comparable to those necessary for a single drilling point with laboratory test campaign. Therefore, limiting drilling to where strictly necessary would strongly reduce the overall cost of the intervention and result in a more effective general understanding of grout efficacy. As an example for the present case study, a single drilling cutting the S-wave velocity anomaly observed in Figure 8d would be more useful than the pre-established drilling points at the corner of the foundation. This approach will have the shortcoming of speeding the testing time when a proper interpretation of geophysical data is available.

Further elaborations of geophysical data by means of properly calibrated correlations between seismic velocity and UCS are also recommended when possible. For the present case study, the heterogeneity of the forming material has strongly limited the applicability of this type of correlations. Because similar conditions are reasonably attended in other case studies, it would also be advisable for an initial testing campaign to be conducted on example grout columns to properly calibrate the data.

6. CONCLUSIONS

Riverbeds characterized by sandy gravels and coarser materials are widespread all over the world. In these areas, bridges on rivers are very common due to high urbanization. Moreover, reports of floods that have damaged or undermined foundations of bridges in these geological conditions are widespread, and jet grouting is one of the most used solutions for such problems.

This work presented a case study on the evaluation of the quality and continuity of jet-grouting injections for bridge scour protection. Direct and indirect tests were performed at four piers of a bridge affected by scour problems. The results from drilling continuous core campaign, seismic surveys, Ultrasonic Pulse Velocity measurements, Point Load and Uniaxial Compressive Strength tests were analyzed and compared.

Even given the different adopted investigation scales and methodologies, it can be stated that the proposed approach, if applied systematically, can have the advantage of reducing the investigation costs and establishing useful correlations between the different measured parameters. Useful

suggestions for testing in similar contexts have also been learned from the present case study. Dealing with the strong material heterogeneity at the site, which is likely to affect rivers with high hydraulic energy causing scour problems, was challenging and required a careful examination of all the acquired data. In similar conditions, a dual approach involving direct tests and indirect investigations is advisable to better understand the different investigation scales.

With respect to the designed intervention for the protection of the specific bridge, it is possible to conclude that, overall, the jet-grouting quality was satisfactory. Only a reduction of compaction has been noticed at the end of some of the injected piles, but as a whole, no particularly relevant anomalies have been noticed in the lateral uniformity of the pile group. This is reflected in the low number of samples (below 15%) having lower material class and UCS properties and in the overall global homogeneity of the seismic surveys.

ACKNOWLEDGMENTS

Surveys of this work have been financed under an agreement between Earth Science Department of University of Torino and Cuneo Provincial Authority. The authors are indebted to Politecnico di Torino for their permission of the use of seismic instrumentation.

REFERENCES

ASTM (2002) Standard Test Method for Laboratory Determination of Point Load Strength Index of Rock. D5731-02, American Society for Testing and Materials, West Conshohocken, Pennsylvania, USA.

ASTM (2008) Standard Test Method for Laboratory Determination of Pulse Velocities and Ultrasonic Elastic Constants of Rock. D2845-08, American Society for Testing and Materials, West Conshohocken, Pennsylvania, USA.

Barkdoll BD, Ettema R, Melville BW (2007) Countermeasures to protect bridge abutments from scour. National Cooperative Highway Research Program, Report No. 587, Transportation Research Board, Washington DC.

Barton N (2007) Rock Quality, Seismic Velocity, Attenuation and Anisotropy. Taylor & Francis, London.

Bowden AJ, Black JL, Ullyott S (1998) Point Load Testing of Weak Rocks with Particular Reference to Chalk. Quarterly Journal of Engineering Geology and Hydrogeology 31: 95-103.

Colombero C, Comina C, Giuliani A, Mandrone G (2016) Ultrasonic equipment aimed to detect grouting homogeneity in geothermal heat exchangers. Proc. European Geothermal Congress 2016, Strasbourg, 19-23 September, T-HP-336.

Croce P, Flora A, Modoni G (2014) Jet Grouting: Technology, Design and Control. CRC Press.

De Falco F, Mele R (2002) The monitoring of bridges for scour by sonar and sediment. NDT & E International 35(2): 117-123.

Deng L, Cai CS (2010) Bridge scour: prediction, modeling, monitoring and countermeasures – Review. Practice Periodical on Structural Design and Construction 15: 125-134.

Gemmi B, Morelli G, Bares FA (2003) Geophysical investigations to assess the outcome of soil modification work: measuring percentile variations of soil resistivity to assess the successful modification of foundation soil by jet grouting. Grouting and Grout Treatment - Proceedings: 1490-1506.

Hayes DC, Drummond FE (1995) Use of fathometers and electrical-conductivity probes to monitor riverbed scour at bridges and piers. Water Resource Investigation Rep. No. 94-4164, U.S. Geological Survey, Hartford, Connecticut.

Jahanger ZK, Azad Abbas A (2013) Correlation Between Point Load Index And Very Low Uniaxial Compressive Strength Of Some Iraqi Rocks. Australian Journal of Basic and Applied Sciences 7(7): 216-229.

Kahraman S, Gunaydin O, Fener M (2005) The effect of porosity on the relation between uniaxial compressive strength and point load index. Int J Rock Mech Min Sci 42(4):584–589. doi: 10.1016/j.ijrmms.2005.02.004.

ISRM (1979) Suggested Methods for Determining Uniaxial Compressive Strength and Deformability of Rock Materials. International Society for Rock Mechanics, Commission on Standardization of Laboratory and Field Tests. International Journal of Rock Mechanics, Mineral Science and Geomechanics 16:135-140.

ISRM (1981) Rock Characterization, Testing and Monitoring: ISRM Suggested Methods. Editor: Brown ET, Pergamon press, 211 pp.

ISRM (1985) Suggested Methods for Determining Point Load Strength.

Lagasse PF, Zevenbergen LW, Schall JD, Clopper PE (2001) Bridge scour and stream instability countermeasures: experience, selection and design guidelines. Federal Highway Administration, Hydraulic Engineering Circular No. 23: FHWA NHI 01-003, U.S. Department of Transportation, Washington DC.

Lytle RJ, Dines KA, Laine EF, Lager DL (1978) Electromagnetic Cross-Borehole Survey of a Site Proposed for an Urban Transit Station. UCRL-52484, Lawrence Livermore Laboratory, University of California.

Millard SG, Bungey JH, Thomas C, Soutsos MN, Shaw MR, Patterson A (1998) Assessing bridge pier scour by radar. NDT & E International 31(4): 251-258.

Padura AB, Sevilla JB, Navarro JG, Bustamante EY, Crego EP (2009) Study of the soil consolidation using reinforced jet grouting by geophysical and geotechnical techniques: “La Normal” building complex (Granada). Construction and Building Materials 23: 1389-1400.

Park I, Lee J, Cho W (2004) Assessment of bridge scour and riverbed variation by a ground penetrating radar. Proceedings 10th International Conference on Ground Penetrating Radar: 411-414, Delft, The Netherlands.

Parker GW, Bratton L, Armstrong DS (1997) Stream stability and scour assessments at bridges in Massachusetts. US Geological Survey Open File Report No. 97-588 (CD ROM), Massachusetts Highway Dept. Bridge Section, Marlborough, Massachusetts.

Peterson JE, Paulson BNP McEvilly TV (1985) Applications of Algebraic Reconstruction Techniques to Crosshole Seismic Data. Geophysics: 50, 1566-1580.

Rucker ML (2006) Surface geophysics as tools for characterizing existing bridge foundation and scour conditions. www.memphis.edu/ce/.

Santarato G, Ranieri G, Occhi M, Morelli G, Fischanger F, Gualerzie D (2011) Three-dimensional Electrical Resistivity Tomography to control the injection of expanding resins for the treatment and stabilization of foundation soils. Engineering Geology 119(1–2): 18–30. doi:10.1016/j.enggeo.2011.01.009.

Singh TN, Kainthola A, Venkatesh A (2012) Correlation between point load index and uniaxial compressive strength for different rock types. Rock Mech Rock Eng 45(2):259–264. doi:10.1007/s00603-011-0192-z.

Sonmez H, Gokceoglu C, Medley EW, Tuncay E, Nefeslioglu HA. (2006) Estimating the uniaxial compressive strength of a volcanic bimrock. Int J Rock Mech Min Sci 43:554–561.

Tucker SE, Briaud JL, Hurlebaus S, Everett ME, Arjwech R (2015) Electrical resistivity and induced polarization imaging for unknown bridge foundations. Journal Geotechnical Geoenvironmental Engineering 141(5): 04015008.

Um J, Thurber CH (1987) A fast algorithm for two-point seismic ray tracing. Bull. Seismol. Soc. Am. 77: 972–986.

Zacoeb A, Ishibashi K (2009) Point Load Test Application for Estimating Compressive Strength of Concrete Structures from Small Core. Journal of Engineering and Applied Sciences 4(7): 46-57.

LIST OF FIGURES

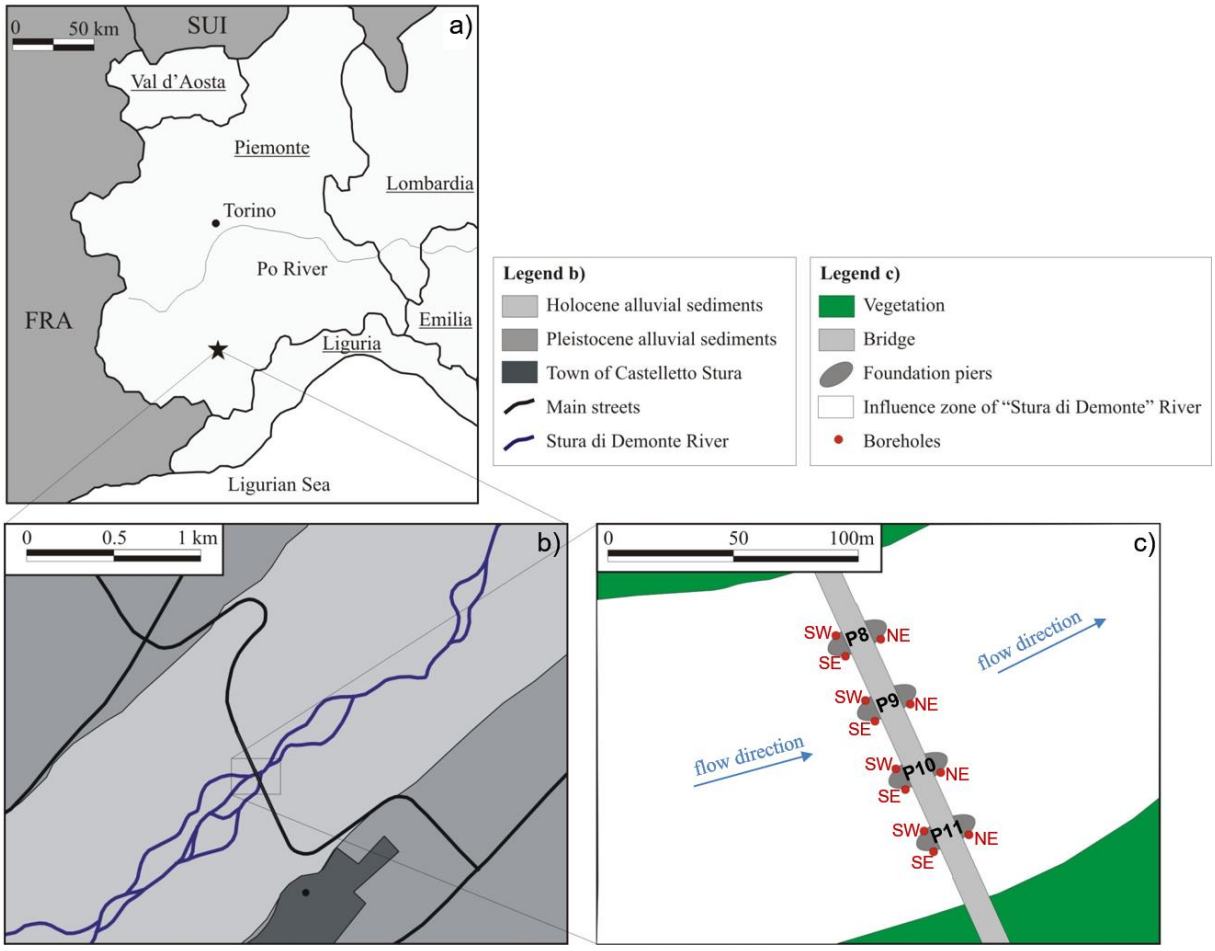

Figure 1 (a) Geographical location of the study area. (b) Geological details of the alluvial deposits of the Stura di Demonte River near the bridge. (c) Detail of the four investigated scored piers (P8 to P11).

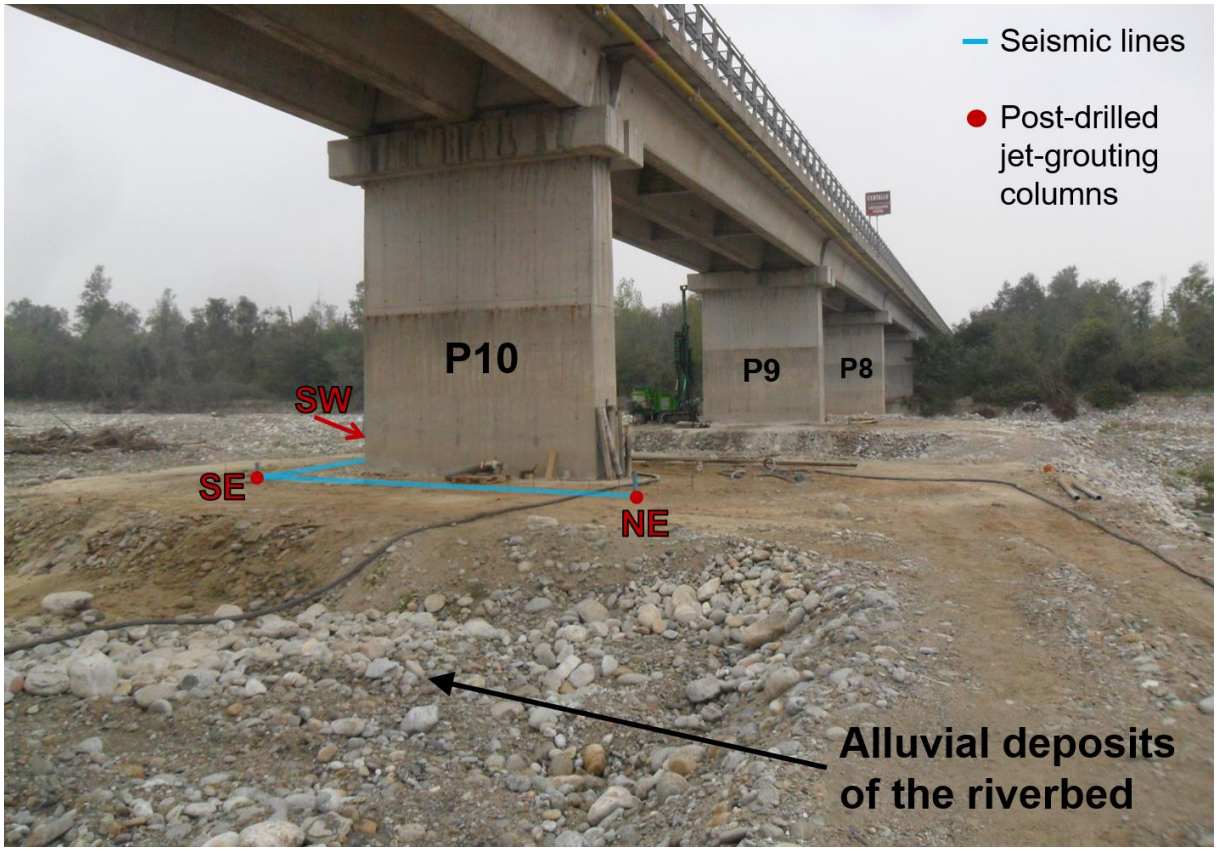

Figure 2 Actual alluvial deposits on the riverbed around the piers of the bridge and completed (P10) or in-progress (P9) jet-grouting interventions on the scoured foundations. Evidences of the post-drilled boreholes used for the surveys and of the imaged seismic sections are also highlighted on P10

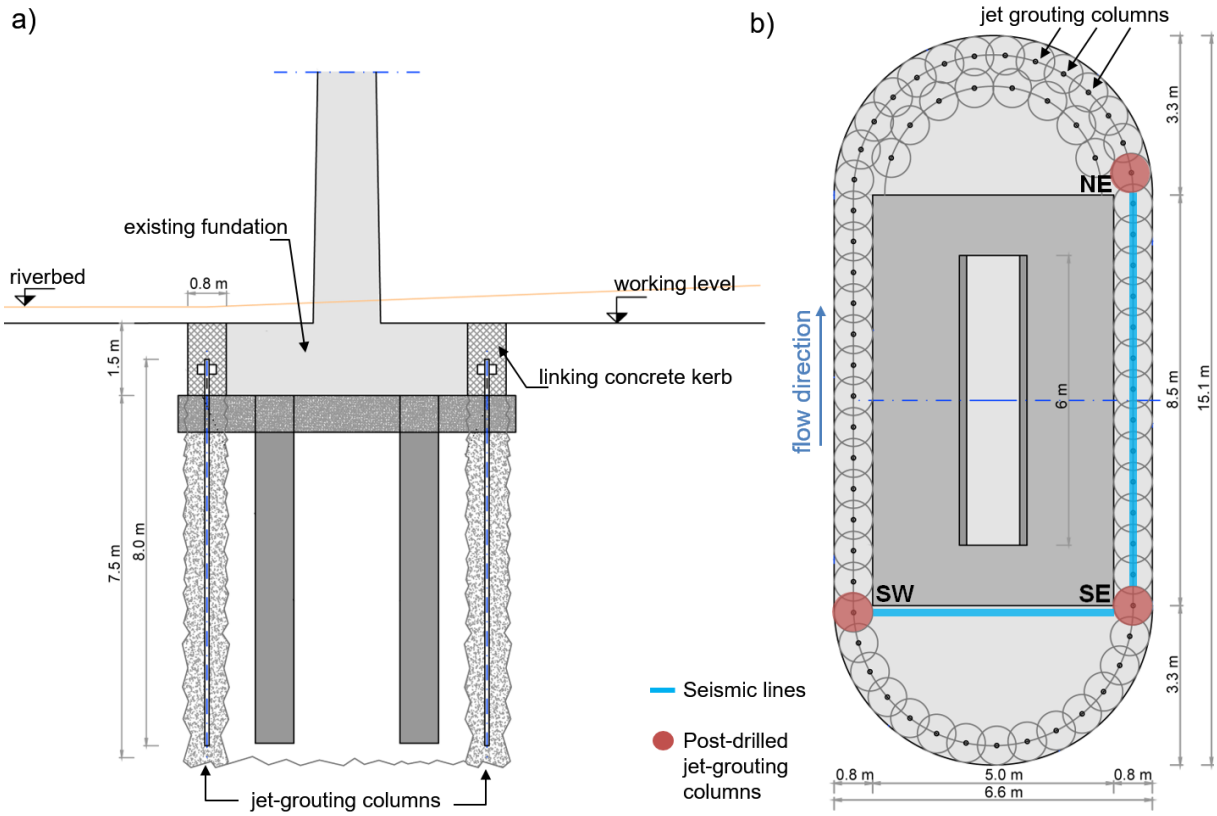

Figure 3 (a) Section and (b) planar view of the designed jet-grouting interventions at each of the four scoured piers of the bridge. Evidences of the post-drilled boreholes used for the surveys and of the imaged seismic sections are also reported in (b).

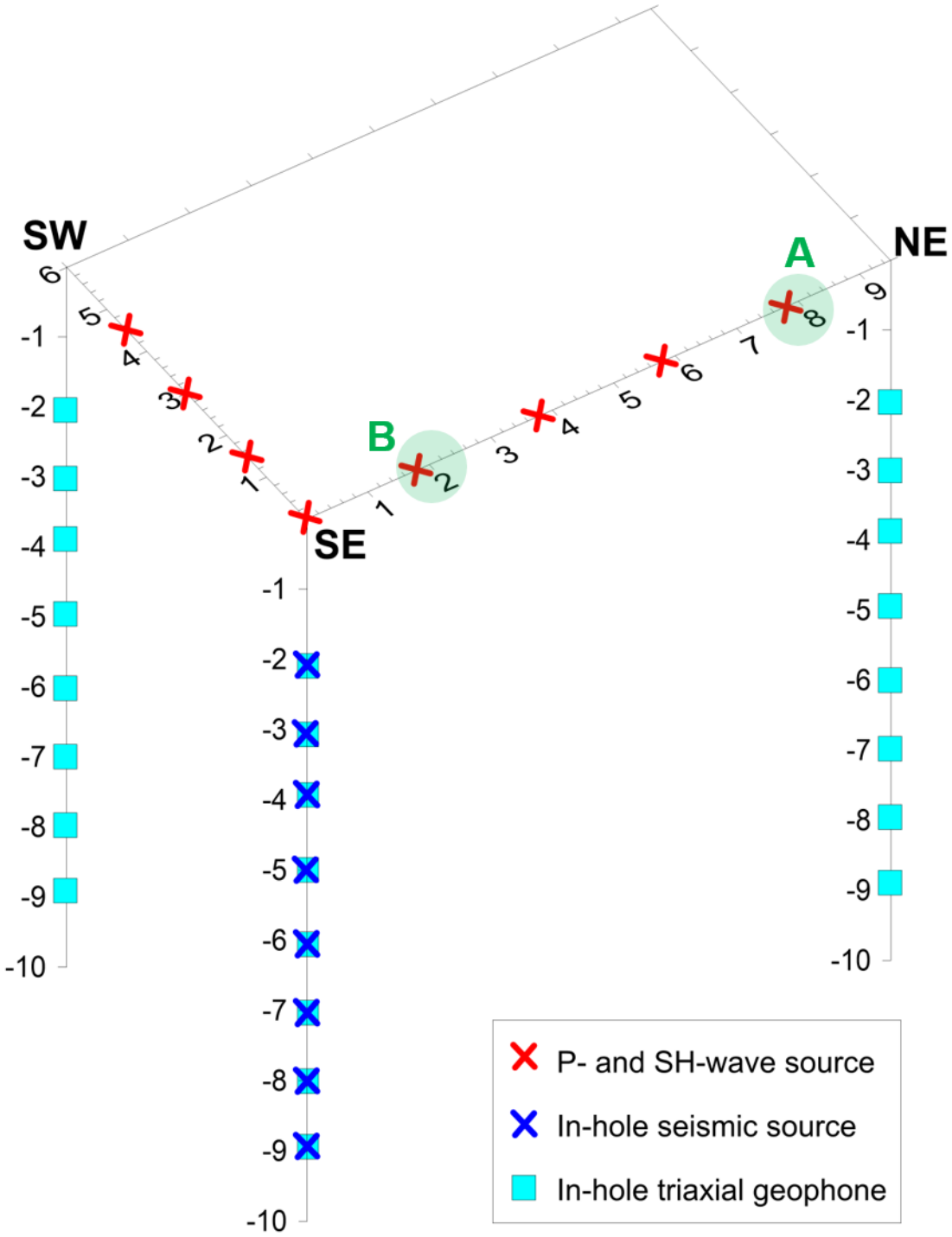

Figure 4 Acquisition scheme for the seismic survey on pier P10, with the location of all the surface and in-hole sources and receivers. Points A and B are the positions of the shots for the seismograms recorded in the NE borehole reported in Figure 5.

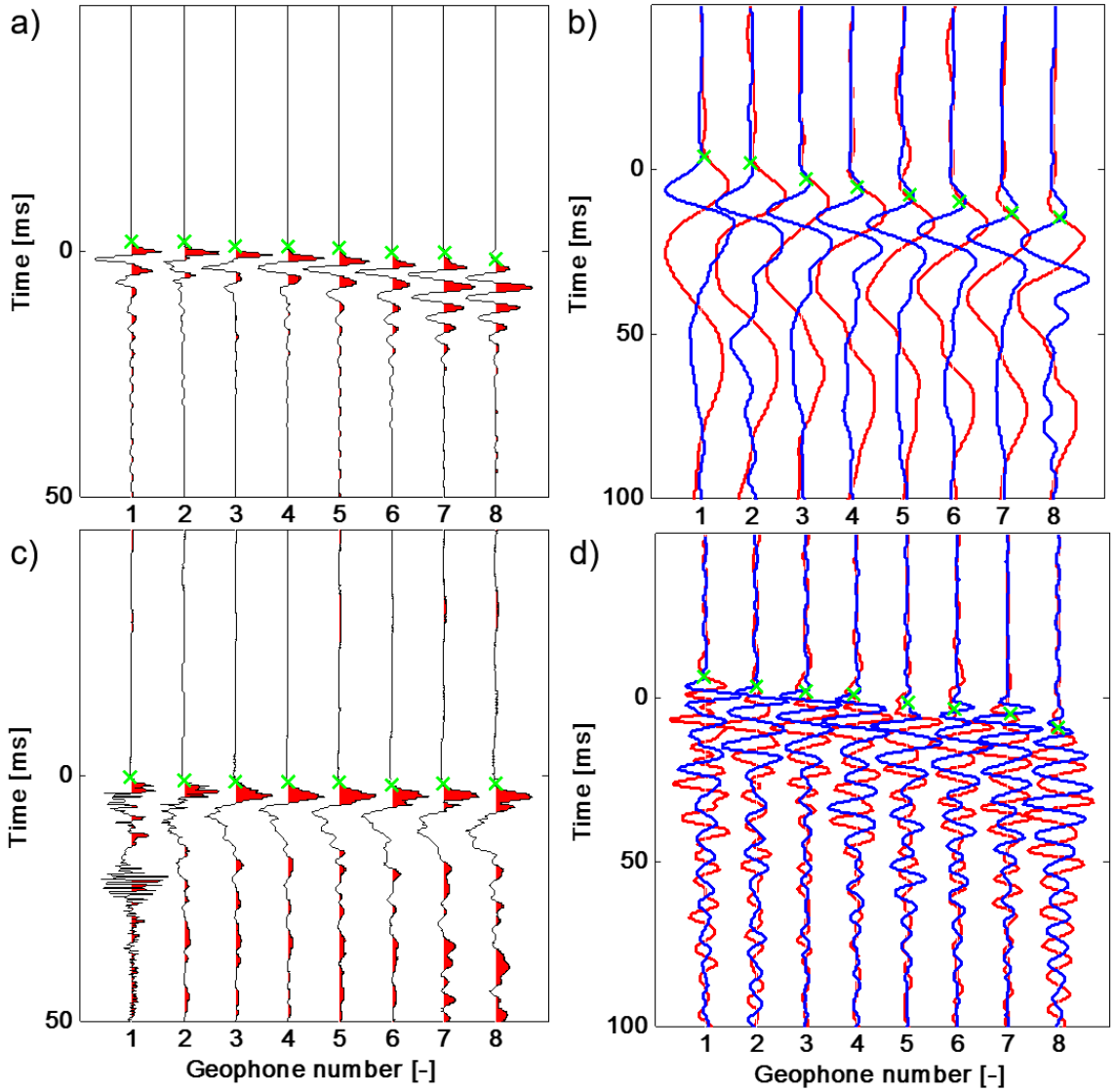

Figure 5 Example of the P- (a, c) and SH-wave (b, d) traces acquired in the NE borehole, with marked first break picking (green crosses). It is possible to observe the deterioration of signal quality from the near shot A (a, b) to the far shot B (c, d), which locations are shown in Figure 4.

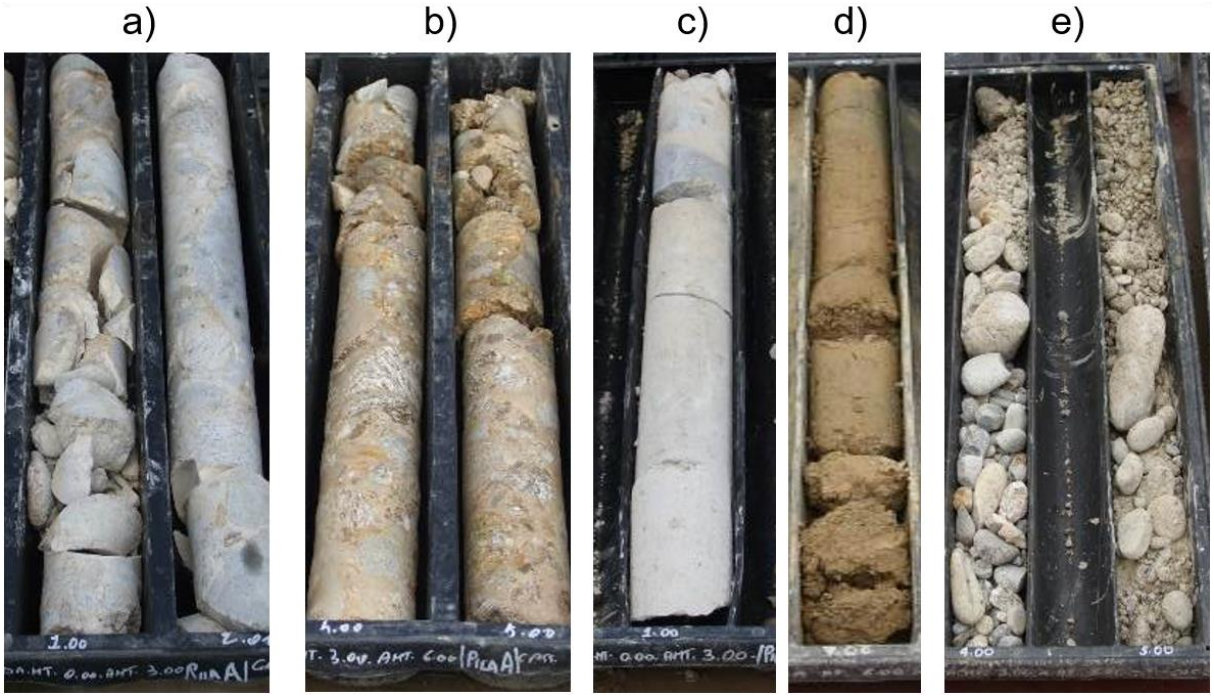

Figure 6 Examples of core drilling assigned to the five material classes: (a) A, (b) B, (c) C, (d) D and (e) E class.

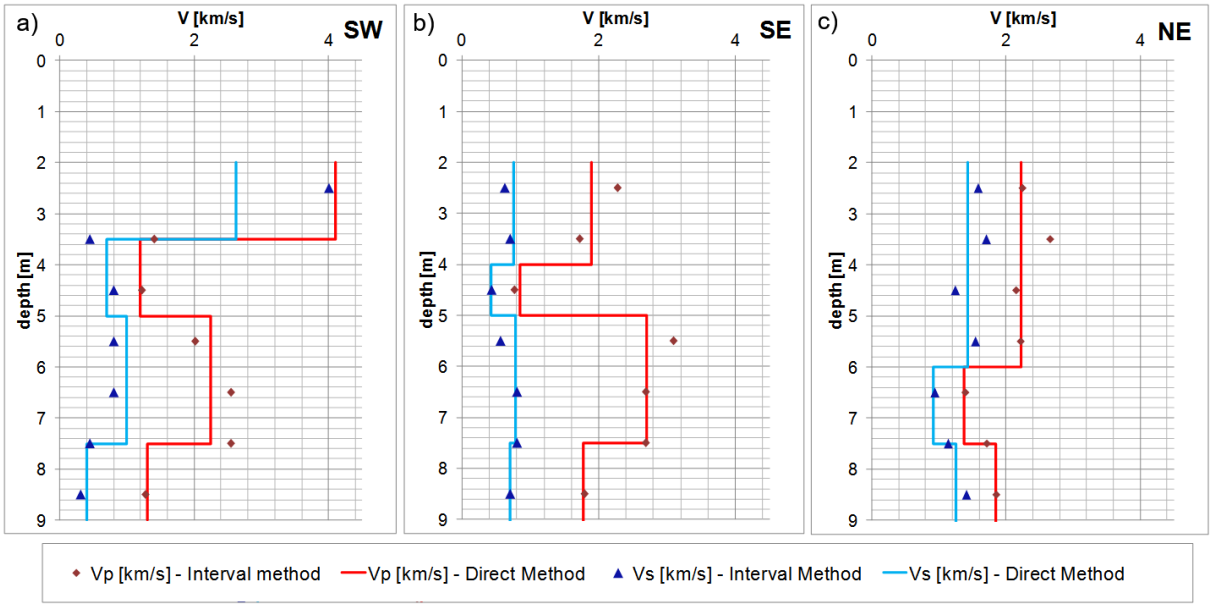

Figure 7 Seismic down-hole interpretation for the boreholes of pier P10: (a) SW, (b) SE, (c) NE borehole.

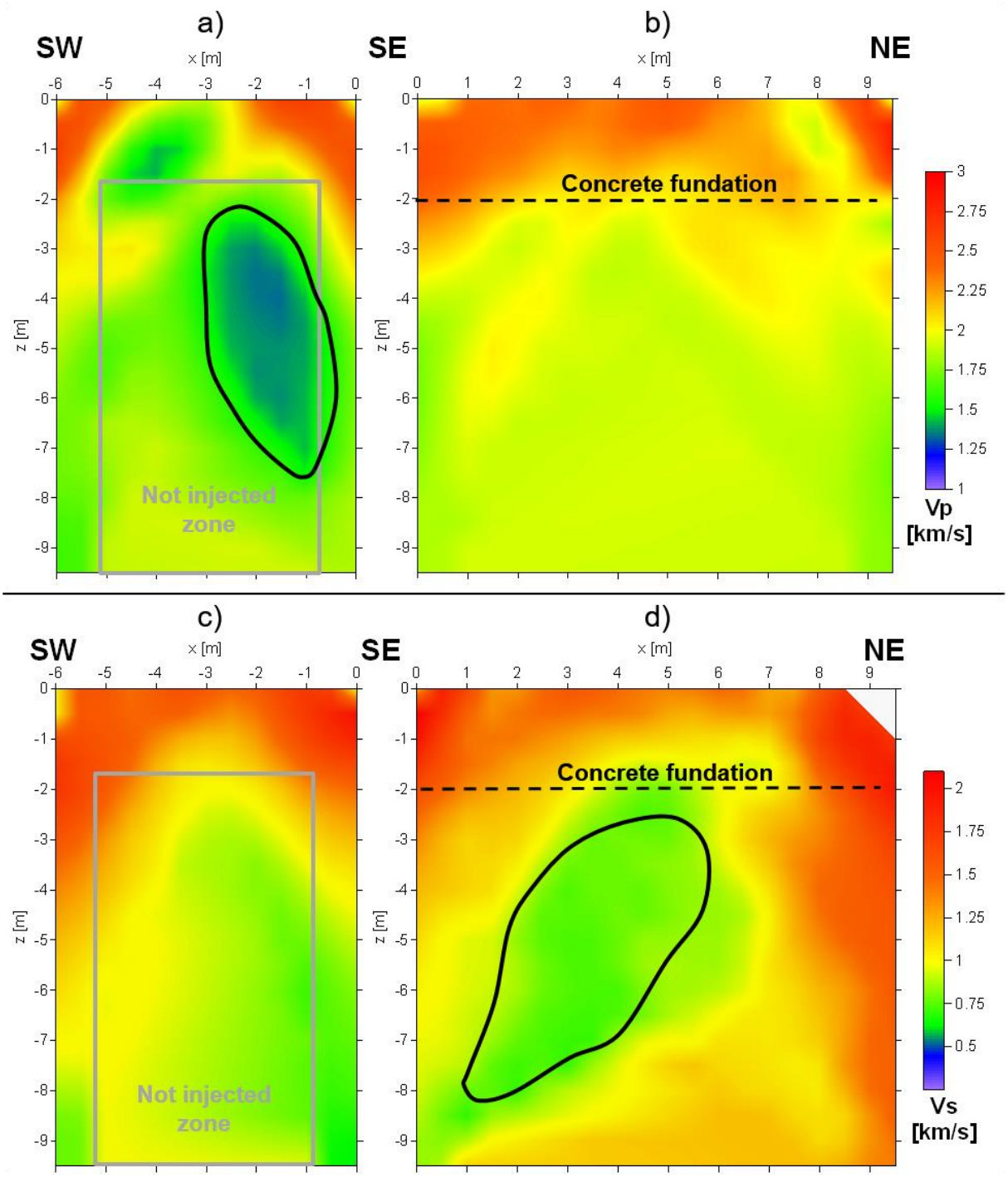

Figure 8 Cross-hole tomographic results on pier P10. For P waves: (a) SW-SE section and (b) SE-NE section. For SH waves: (c) SW-SE section and (d) SE-NE section.

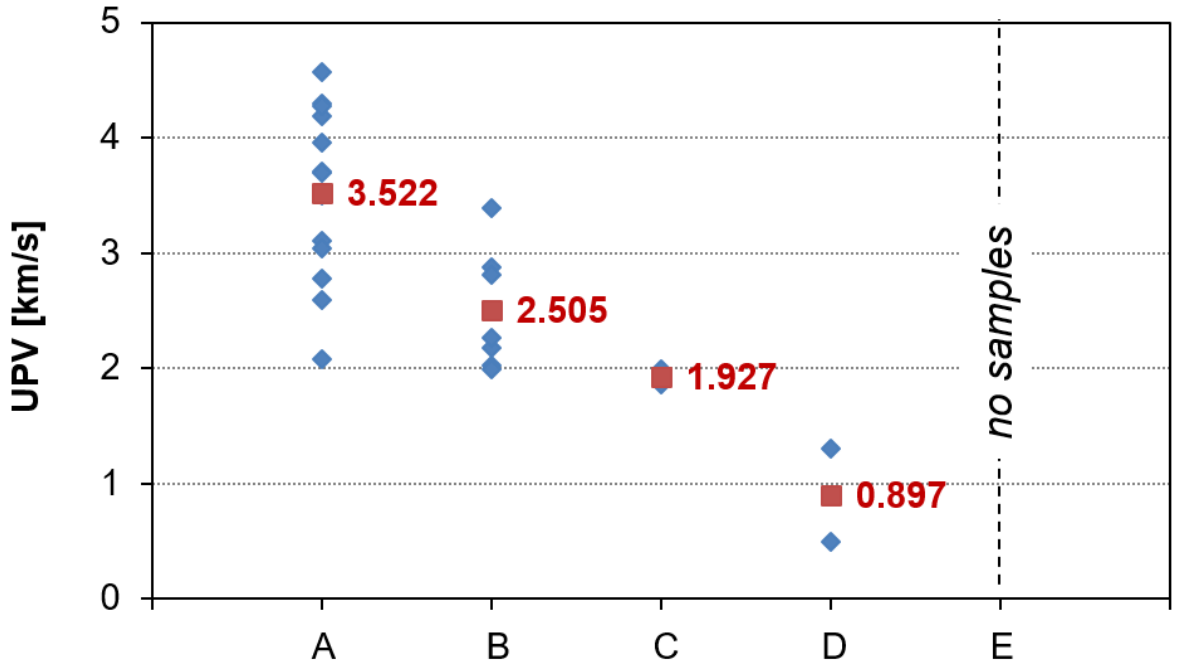

Figure 9 Ultrasonic Pulse Velocity (UPV) measurements on samples of the different material classes; the mean value of each class is reported in red.

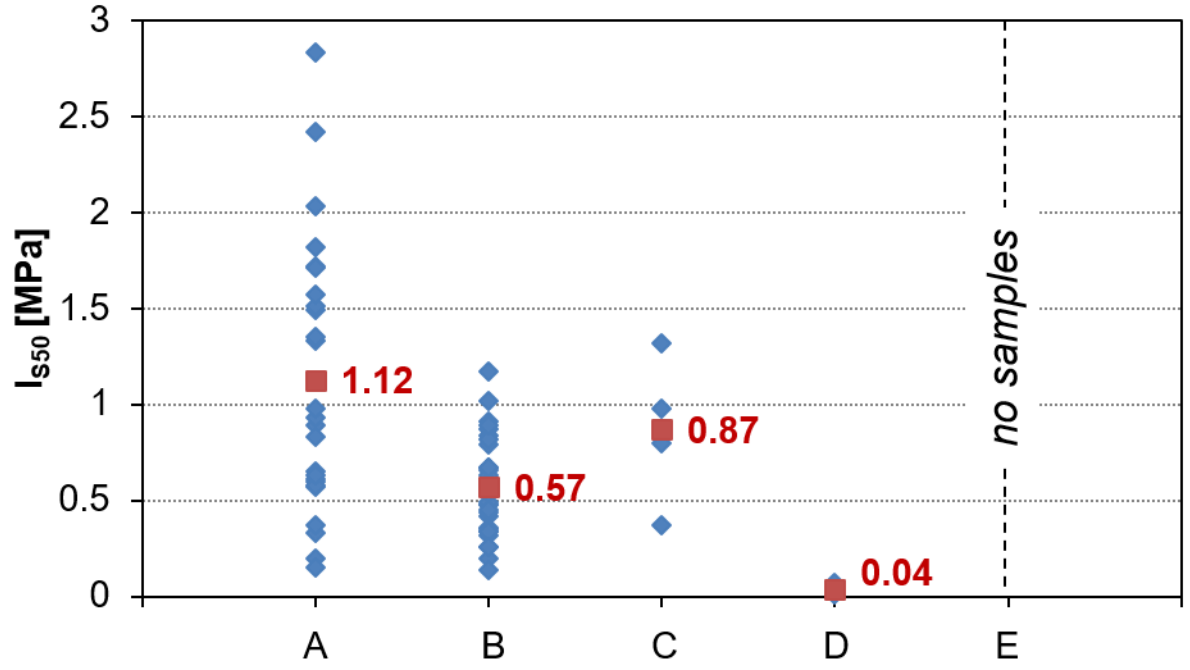

Figure 10 I_{S50} values obtained from the Point Load Test on samples of the different material classes; the mean value of each class is reported in red.

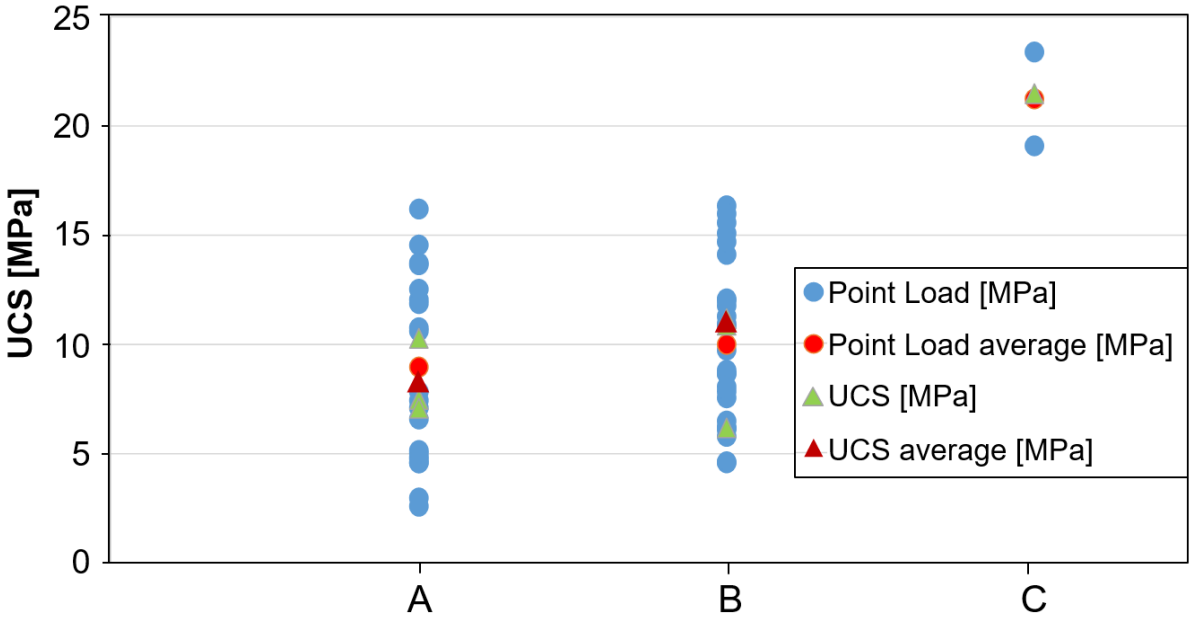

Figure 11 UCS values obtained from Point Load Test and direct Uniaxial Compressional tests on samples of the different material classes (A to C) with related average values.

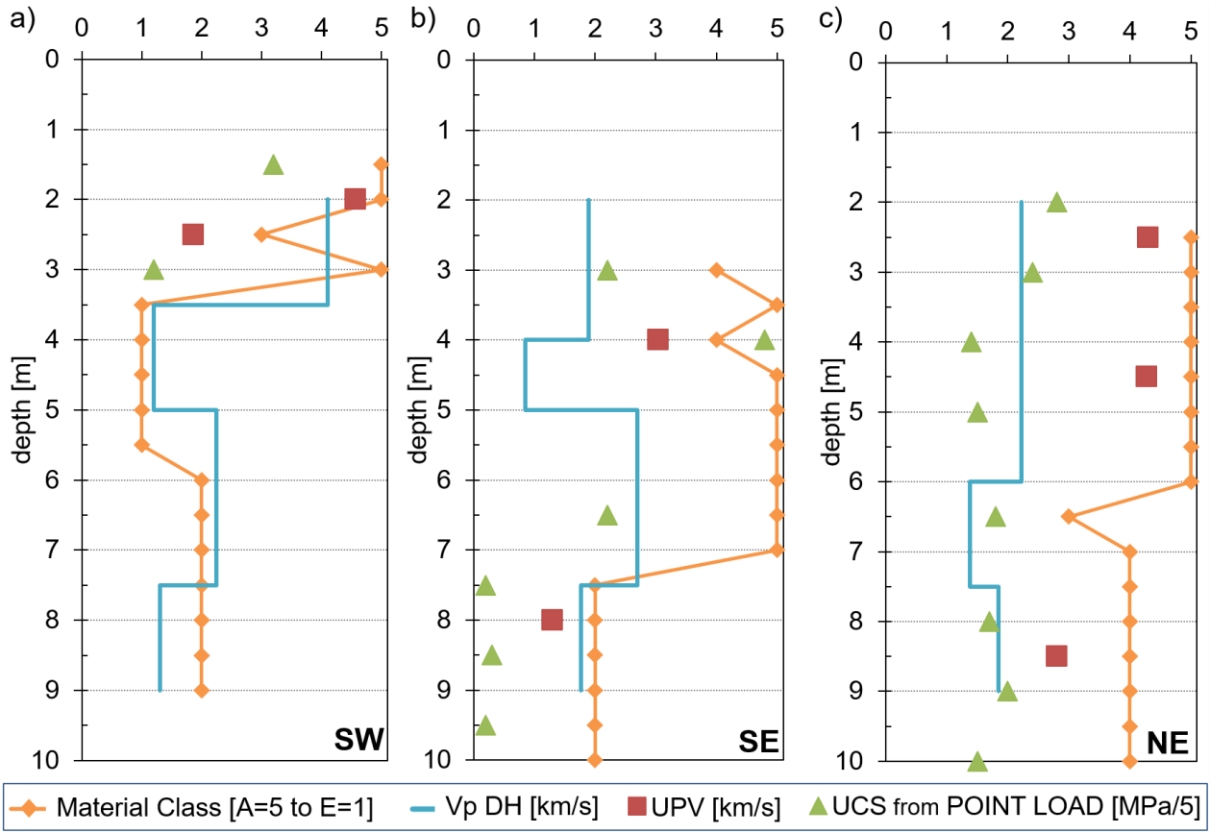

Figure 12 Comparison of the results yielded by both field and laboratory tests for pier P10. The material class has been converted to numerical values starting from best quality (A=5) to worst (E=1), while the UCS values from Point Load tests have been divided by 5. (a) SW, (b) SE, (c) NE borehole.

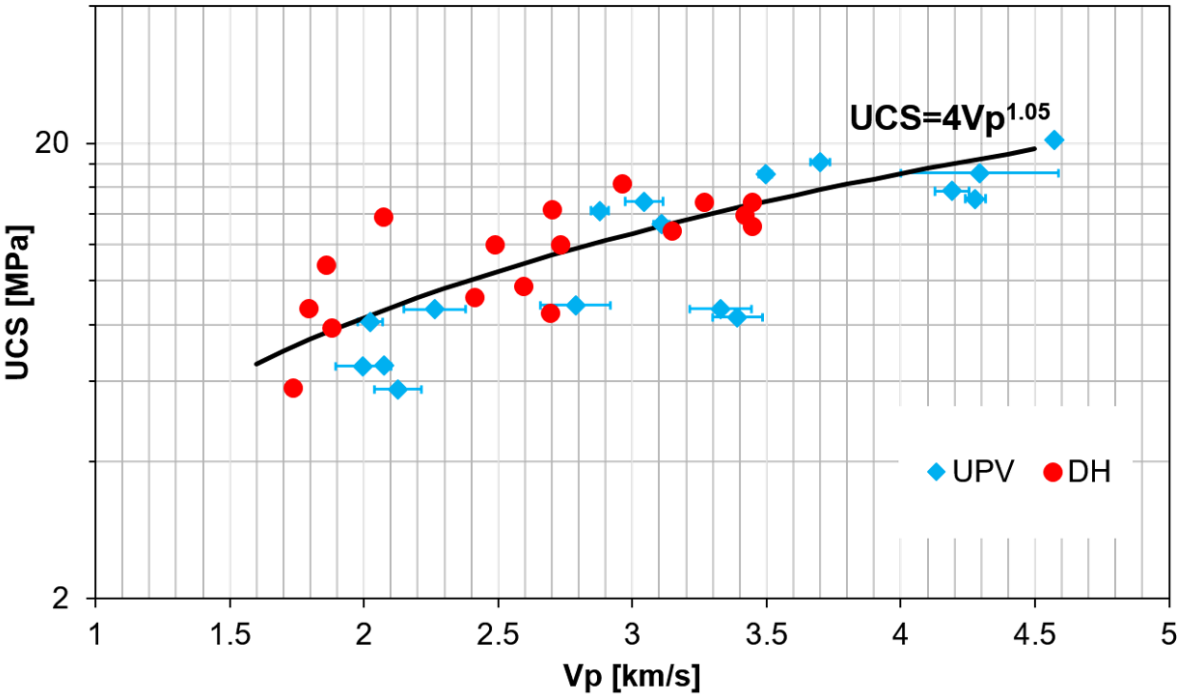

Figure 13 Correlation between measured seismic velocities (from down-hole and UPV tests) and Uniaxial Compressive Strength (UCS) for material classes A and B.